NASA/TM–20220002988

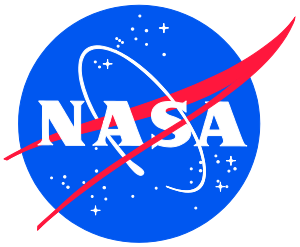

Thermocouple Temperature Measurements in Selective Laser Melting Additive Manufacturing

Alexandra M. Vest, David R. St-Pierre, Stephen Rock, Antoinette M. Maniatty,and Daniel J. Lewis
Rensselaer Polytechnic Institute, Troy, New York

Samuel J.A. Hocker
Langley Research Center, Hampton, Virginia

March 2022

NASA STI Program Report Series

Since its founding, NASA has been dedicated to the advancement of aeronautics and space science. The NASA scientific and technical information (STI) program plays a key part in helping NASA maintain this important role.

The NASA STI program operates under the auspices of the Agency Chief Information Officer. It collects, organizes, provides for archiving, and disseminates NASA's STI. The NASA STI program provides access to the NTRS Registered and its public interface, the NASA Technical Reports Server, thus providing one of the largest collections of aeronautical and space science STI in the world. Results are published in both non-NASA channels and by NASA in the NASA STI Report Series, which includes the following report types:

- TECHNICAL PUBLICATION. Reports of completed research or a major significant phase of research that present the results of NASA Programs and include extensive data or theoretical analysis. Includes compilations of significant scientific and technical data and information deemed to be of continuing reference value. NASA counterpart of peer-reviewed formal professional papers but has less stringent limitations on manuscript length and extent of graphic presentations.

- TECHNICAL MEMORANDUM. Scientific and technical findings that are preliminary or of specialized interest, e.g., quick release reports, working papers, and bibliographies that contain minimal annotation. Does not contain extensive analysis.

- CONTRACTOR REPORT. Scientific and technical findings by NASA-sponsored contractors and grantees.

- CONFERENCE PUBLICATION. Collected papers from scientific and technical conferences, symposia, seminars, or other meetings sponsored or co-sponsored by NASA.

- SPECIAL PUBLICATION. Scientific, technical, or historical information from NASA programs, projects, and missions, often concerned with subjects having substantial public interest.

- TECHNICAL TRANSLATION. English-language translations of foreign scientific and technical material pertinent to NASA's mission.

Specialized services also include organizing and publishing research results, distributing specialized research announcements and feeds, providing information desk and personal search support, and enabling data exchange services.

For more information about the NASA STI program, see the following:

- Access the NASA STI program home page at http://www.sti.nasa.gov

- Help desk contact information:

https://www.sti.nasa.gov/sti-contact-form/
and select the "General" help request type.

NASA/TM–20220002988

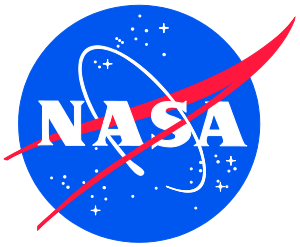

Thermocouple Temperature Measurements in Selective Laser Melting Additive Manufacturing

Alexandra M. Vest, David R. St-Pierre, Stephen Rock, Antoinette M. Maniatty, and Daniel J. Lewis
Rensselaer Polytechnic Institute, Troy, New York

Samuel J.A. Hocker
Langley Research Center, Hampton, Virginia

National Aeronautics and
Space Administration

Langley Research Center
Hampton, Virginia 23681-2199

March 2022

Available from:

NASA STI Program / Mail Stop 148
NASA Langley Research Center
Hampton, VA 23681-2199
Fax: 757-864-6500

Table of Contents

1.0 Introduction 1
2.0 Methods 3
2.1 Circuitry 3
2.2 SLM Machine 4
3.0 Results 6
4.0 Conclusions and Recommendations 7
Acknowledgements 10
References 11

List of Figures

Figure 1. Breadboard combining the AD8495 thermocouple amplifier with the Teensy® 3.5 for data acquisition. The thermocouple wires feed directly into the AD8495 thermocouple amplifiers. The IR photodiode allows for data synchronization with the laser. 3

Figure 2. Flowchart of the data acquisition process. 4

Figure 3. (a) Close-up image of spot welded thermocouple junction in the machined well on the build plate. (b) Three thermocouples spot welded into machined wells on the build plate. Wire protruding from the build plate run to the circuitryboard. 5

Figure 4. Laser tracks on the build plate relative to the three thermocouples. 6

Figure 5. Reading from thermocouple 1, from test set 2, with a laser power of 170 W, velocity of 500 mm/s, and varying distance from the thermocouple channel. 7

Figure 6. Readings from thermocouples 1 and 2 from test set 6, with a laser power of 400 W, laser speed 2100 mm/s, hatch spacing of 30 μm, and initial and final distances of approximately 900 µm and 30 μm from the thermocouple weld junctions. 8

Figure 7. Detail of the highest temperature peak recorded by thermocouple 1 for the same case as shown in Figure 6. The red section shows the data points (circles) during the temperature rise. 8

Figure 8. Detail of the final peak from test set 6 (laser speed 2100 mm/s, hatch spacing 30 μm) at different power levels 9

Figure 9. Thermocouples spot welded to the top edge of a 50.8 mm 25.4 mm 6.35 mm Inconel 718 build plate for future work. 9

Figure 10. Fixtures for ensuring accurate location of thermocouple weld placement on the build plate. 9

List of Tables

Table 1. Sets of test case conditions (TC = thermocouple). 6

Nomenclature

μm	micrometer
Hz	hertz
in	inch
kHz	kilohertz
mm/s	millimeters per second
nm	nanometers
W	Watts

CCD	charge-coupled device
IR	infrared
SLM	selective laser melting
TC	thermocouple

Abstract

The extreme thermal history resulting from selective laser melting leads to microstructural characteristics and residual stresses that have considerable impact on the mechanical behavior of the printed part. Accurate measurements of the temperature combined with thermal models are needed to better understand and control the thermal history to optimize mechanical properties. In order to calibrate and validate models, experimental temperature data must be accurately measured in a rapid fashion due to the high speeds of the laser. In this work, a novel method to read data from thermocouples is created with enhanced circuitry that achieves a sampling rate of 10 kHz. This data acquisition rate allows for high precision sampling of SLM heating and cooling cycles.

1.0 Introduction

The rapid heating and cooling cycle, typical in selective laser melting (SLM) additive manufacturing, creates non-equilibrium microstructures and potentially high residual stresses, which directly impact the mechanical properties [1]. Accurate temperature field histories are required to provide insight into the development of microstructures and residual stresses during laser passes, which may be used for process control and optimization. While there has been substantial work in developing SLM process models to predict the temperature field history, due to the complex physics of material-laser interaction, phase change, and consolidation, these models are not fully predictive and require calibration against accurate experimental data [2][3]. Experiments that provide accurate, but sparse temperature data combined with high-fidelity simulations that provide full field data can provide the data and insight necessary to model the microstructure evolution, to predict residual stresses, and ultimately, to control process parameters to optimize mechanical properties.

Accurate temperature measurements are extremely challenging because the interaction time between the laser and the powder is on the order of milliseconds. Within this time, the powder melts and rapidly resolidifies after the laser leaves the vicinity. Sampling rates must be sufficient to capture this short duration. In addition, the temperature varies tremendously at any given location, from an ambient temperature as low as 20°C to exceeding the melt temperature, upwards of 2000°C, as the laser moves. The extreme temperatures reached during these times are crucial to record as they give information pertinent to phase-change and microstructure evolution.

There has been considerable effort to develop methods to overcome the challenges to monitor the temperature field during SLM (or more generally powder-bed fusion additive manufacturing). The modalities for measuring temperature can be categorized as non-contact and contact methods. The non-contact methods include using infrared cameras, pyrometers, and other optical sensors. Non-contact, optical methods have the advantage of being able to directly monitor the surface of the melt zone, but typically can only provide a qualitative temperature field over the wide range of interest. In addition, the optical image can be adversely impacted by state dependent and rapidly evolving emissivity, the irregular surface topology, and ejected particles and vapor in the chamber. Thermocouples are a principal contact method and typically provide more accurate measurements

and are considerably less expensive but require careful placement. Each contact measurement returns the temperature at a single location and cannot monitor directly in the melt zone. Obtaining the high sampling rates that are characteristic of the SLM process is a challenge for all modalities.

Infrared (IR) cameras are frequently used for their relatively quick data acquisition. Standard IR cameras are reported with frame rates up to 6.3 kHz [4], which approaches the frame rate required to capture the rapid temperature cycle in SLM. In-situ IR cameras require extra shielding to protect them from gas and debris arising from the process [5]. Kapton film may be used for protection from the stray particles; however, metallization of the Kapton film may occur causing inaccuracy in the signal read from the IR camera [6]. The location of the camera relative to the laser may also limit the detection area [7][8]. The SLM process challenges IR cameras to measure high quality optical images and in relating the measured IR intensities to an accurate temperature field.

It is extremely difficult to relate the IR intensity to an accurate temperature field because the emissivity varies substantially over the large temperature range, and thus, IR cameras typically provide only qualitative temperature data [5]. The variable surface topography also impacts the image quality. Raplee *et al.* make a calibration profile for in-situ IR cameras to account for these emissivity and topography changes that occur during electron beam manufacturing to interpret the transient layer temperature of the part during and after melting with limited success [6]. In that work, several discrepancies arise including some regions displaying temperatures cooler after melting than before the laser passed due to the need to switch between multiple calibration curves. To increase the range of temperatures that can be accurately measured, Hooper uses a two-camera set-up with dissimilar wavelengths to eliminate the need to account for the changing emissivity [9]. Using a silicon-based sensor, temperatures within the 1000–4000 K range are imaged at a frame rate of 100 kHz and are found to be within 1% of thermocouple measurements taken within the system for a majority of the heating. Lower temperatures cannot be imaged accurately with this system and would require non-silicon sensor technology that would also limit the frame rate.

While IR cameras measure the temperature distribution over an area, there are also non-contact sensor modalities that measure the temperature along a line and pyrometers that return a single temperature over a circular spot. Devesse *et al.* captured accurate temperatures (within 10%) at a rate of 1 kHz within a melt pool of AISI 316L stainless steel using a hyperspectral line camera [10]. As with the IR cameras, due to the temperature dependent emissivity, the recorded temperatures were only accurate over a narrow temperature range, and lower temperatures could not be accurately measured. Pavlov *et al.* utilized a two-wavelength pyrometer set up coaxial to the laser path to measure the temperature history in the melt pool in a SLM system [11]. The temperature range of the pyrometer was limited to 900–2600°C, and due to the steep temperature gradients in the observed region, it is unclear the meaning of the single measured temperature. Chivel and Smurov report using a charge-coupled device (CCD) camera in conjunction with pyrometers to monitor temperature profiles compatible with the wavelengths of the camera and the maximum temperature, but instabilities were observed in the system that are attributed to the laser movement in and out of the field of view [12].

Thermocouples offer a relatively inexpensive way to record the temperature at a single location. In Rodriguez *et al.*, thermocouples are used in addition to IR cameras to provide an accurate temperature reading at a specific location within the build, where the thermocouples are inserted into a hole drilled into the build, already several layers deep [5]. Masoomi *et al.* attempted to use thermocouples to validate SLM simulations but was unsuccessful due to the slow frame rate of

their thermocouple system [13]. In Chiumenti *et al.*, thermocouples are embedded in the build plate to measure the temperature at locations near the melt region, in order to validate the simulation prediction of the temperature history at these locations [14]. The sampling rate in that work is reported to be 1 kHz, and the data is observed to be very sparse, not capturing the fast heating, and noisy.

In this paper, a novel, low cost method is described for fast data acquisition of accurate thermocouple temperature measurements within an SLM system. Each thermocouple is spot welded onto a build plate and used within an SLM machine to measure temperature data on the plate as the laser passes. The thermocouples are fed into a thermocouple amplifier. The amplifiers are connected to circuitry which allows for the synchronized and rapid acquisition of temperature data to be stored on an SD card for later analysis.

2.0 Methods

2.1 Circuitry

The prototype circuit is shown in Figure 1 and a flowchart of the data acquisition is provided in Figure 2. The circuit is located inside the build chamber. Each of the thermocouples used in the experiment is connected to the AD8495 K-type thermocouple differential input amplifier on a custom board with cold junction compensation. Further details of the custom board, including a circuit diagram and associated code is given in [15]. A Teensy® 3.5 microcontroller is integrated to receive the three thermocouple signals. The Teensy® 3.5 then saves the data to an SD memory card in a BIN file that is later transferred to a computer for analysis. The data is then read into software where the data may be refined with digital noise reduction filters. For data synchronization, an IR photodiode is also mounted on the breadboard to sense when the laser is on. Data synchronization is necessary for relating the temporal thermocouple measurement to laser power and position.

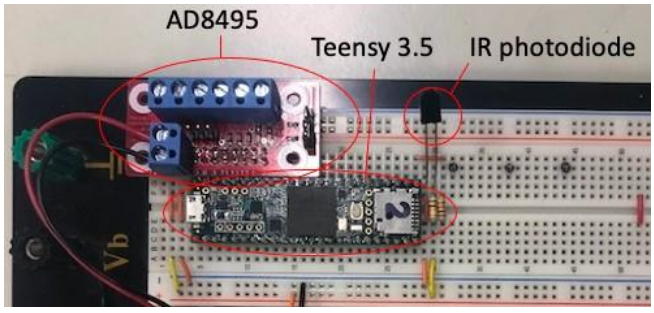

Figure 1. Breadboard combining the AD8495 thermocouple amplifier with the Teensy® 3.5 for data acquisition. The thermocouple wires feed directly into the AD8495 thermocouple amplifiers. The IR photodiode allows for data synchronization with the laser.

Previously, a MAX 31855 digital thermocouple amplifier was used to catalog temperature, but this was observed to limit the frequency of readings to 13 Hz due to limited bandwidth. The upgrade to the analog AD8495 increases the frequency to the 10 kHz seen in these experiments. A Teensy® 3.2 development board was also used in an earlier test but was found to limit the data acquisition rate to 1 kHz.

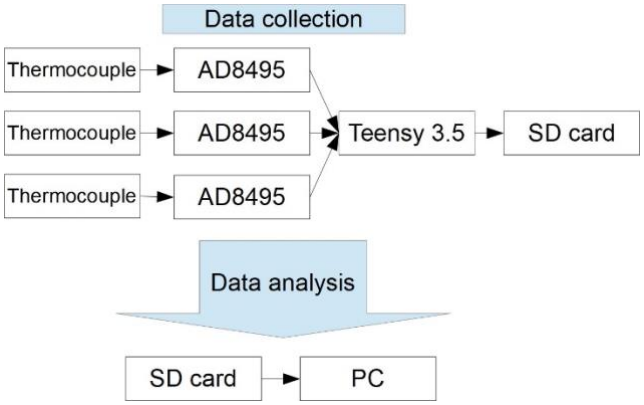

Figure 2. Flowchart of the data acquisition process.

2.2 SLM Machine

An open-architecture SLM machine is used for these experiments. The SLM system was developed under an America Makes grant (Project 4051) at Rensselaer Polytechnic Institute [16], which was a partnership between Rensselaer and GE Global Research Center, with additional support from Empire State Development/NYSTAR. The machine operates using America Makes open-source software (Project 4039) [17]. The system operates within a vacuum chamber with atmospheric control and oxygen ppm level sensing capabilities. It is equipped with a 400W IPG Photonics fiber laser (1070 nm wavelength), a SCANLAB IntelliSCANde 20 galvanometer scanner, and a Sill Optics S4lFT1420 focusing lens to provide a flat focus plane. Powder is applied with a silicone blade spreader. A more detailed description of the system may be found in Shkoruta *et al.* [17] .

In the experiment, three thermocouples are spot welded to the top face of the stainless-steel build plate within small, machined channels as shown in Figure 3(a). The build plate is approximately 50.8 mm × 50.8 mm × 12.7 mm (2 in × 2 in × 0.5 in) (see Figure 3(b)). Three K-type chromel thermocouples of diameter 0.127 mm (0.005 in) are used. The channels protect the thermocouples from the blade spreader when powder is applied. Mounting the thermocouples in blind wells under the build plate was also considered; however, that would have resulted in much greater uncertainty in the exact location of the thermocouples as well as uncertainty as to which surface is in best contact with the junction. Each weld is created using a Unitek spot welder at 10 J. Excess wire is then removed with a razor blade with pressure applied towards the build plate.

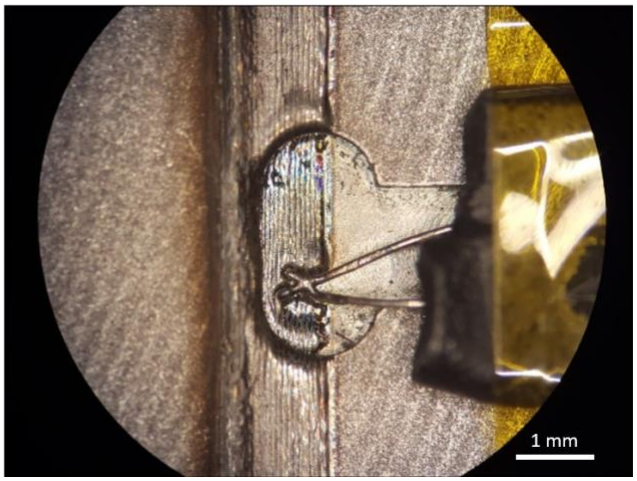

(a)

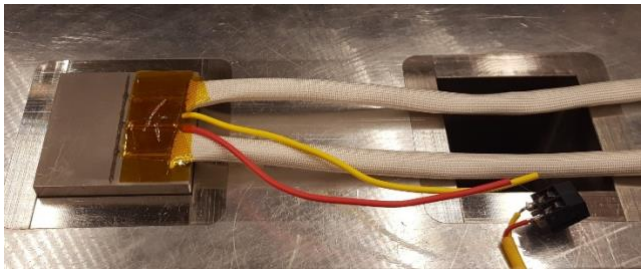

(b)

Figure 3. (a) Close-up image of spot welded thermocouple junction in the machined well on the build plate. (b) Three thermocouples spot welded into machined wells on the build plate. Wire protruding from the build plate run to the circuitry board.

Six sets of test cases are studied, and the conditions are summarized in Table 1. In all cases, the laser travels along the length of the build plate passing at an equal perpendicular distance (for any given pass) from each of the three thermocouple welds (see Figure 4). No powder is applied in any of the test cases presented here. The purpose of the test set 1 is to test the ability to read the rapidly changing temperature at each thermocouple during a single laser pass at varying laser powers (100–300 W) and speeds (150–600 mm/s). Test set 2 is carried out at a constant laser power of 170 W and speed of 500 mm/s. Each test is a single pass, and nine tests are conducted with the distance of the laser track from the thermocouples decreasing approximately 100 μm in each subsequent test, with the laser track being at the edge of the thermocouple channel in the final test.

The next four sets of tests examine the effect of hatch spacing, laser speed, and power on the recorded temperatures. In each case, the laser is moving closer to the thermocouples with each pass, and the laser always travels in the same direction. In test sets 3 and 4, the power (170 W) and speed (500 mm/s) are held constant, and the hatch spacing is varied from 70 µm to 160 μm. During test set 3, the peak temperature is observed to be clipped by the circuit. Subsequently, the circuit is corrected to allow for higher peak temperatures, and test set 4 considers the same set of conditions as test set 3. In test set 5, the power is held constant (170 W), and both the speed (500–2100 mm/s) and hatch spacing (30-130 μm) are varied, where higher speeds are paired with lower hatch spacing. In test set 6, the speed (2100 mm/s) and hatch spacing (30 μm) are held constant, and the power is varied from 200 W to 400 W.

Table 1. Sets of test case conditions (TC = thermocouple).

Set	Power (W)	Speed (mm/s)	Distance from TC	Hatch Spacing (μm)
1	Varied	Varied	Constant	N/A
2	170	500	Varied	N/A
3	170	500	N/A	Varied
4	170	500	N/A	Varied
5	170	Varied	N/A	Varied
6	Varied	2100	N/A	30

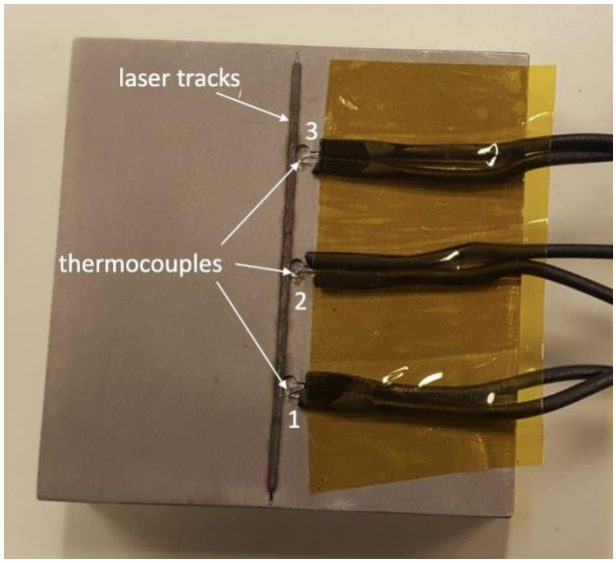

Figure 4. Laser tracks on the build plate relative to the three thermocouples.

3.0 Results

In all tests, a sampling rate of 10 kHz is achieved. In test set 3, thermocouple 3 is damaged by the laser. The other two thermocouples are operational for the remainder of the experiments; however, thermocouple 2 consistently reads lower temperatures. The weld for thermocouple 2 is larger in diameter than the weld for thermocouple 1. This increase in surface area will absorb more heat causing a decrease in the temperature read by the thermocouple [19]. Thus, most of the data presented will be for thermocouple 1. A subset of the data is presented here to highlight the capabilities. The full set of results can be found in [20].

Results from test set 2 are shown in Figure 5, showing the temperature history from single passes of the laser at varying distances from the thermocouple. The temperature histories are well defined. The readings from this set show steeper and higher peaks as the laser passes closer to the thermocouple, and a gradual temperature drop after the laser has passed.

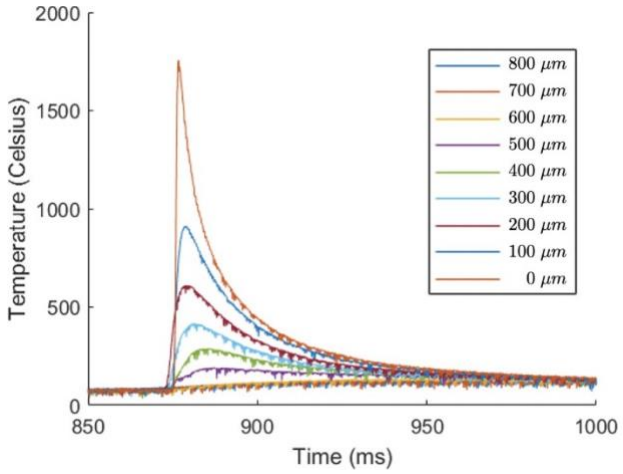

Figure 5. Reading from thermocouple 1, from test set 2, with a laser power of 170 W, velocity of 500 mm/s, and varying distance from the thermocouple channel.

The primary focus of this work is on demonstrating the ability to sample temperature data fast enough to observe temperature histories relevant to SLM; therefore, data from test set 6, at the highest laser speed, is the most relevant. Figure 6 and Figure 7 show results for the laser speed of 2100 mm/s at the peak power of 400 W. In Figure 6, the lower temperature recorded by thermocouple 2, as described earlier, is shown. It is evident in Figure 7 that the data acquisition rate is sufficiently fast to record a well-defined temperature history at thermocouple 1, even at this fast laser speed. In Figure 6, all 30 peak temperatures in each laser pass as the laser approaches the thermocouple are captured as well as the gradual increase in average temperature with each pass.

In Figure 8, the effect of the power on the final (highest) peak from test set 6 is shown. The general trend is an increase in temperature with an increase in power, as expected.

4.0 Conclusions and Recommendations

A method is presented and demonstrated that allows for temperature data to be sampled at a rate of 10 kHz at thermocouples welded to a build plate, which is shown to be sufficient to sample the temperature history during a typical laser pass in an SLM additive manufacturing process. This system can be used for monitoring the temperature history during a SLM build process, which can provide insight to models as well as serve as a tool for model validation studies. A key aspect of this work is the design of a novel circuitry, which allows for the fast-sampling rate. In addition to the fast data acquisition, the method has the advantage of being low cost. Several sets of test conditions are considered to explore the effect of process parameters—power, laser speed, and hatch spacing—on the temperature history. The data recorded follows expected trends; however, the accuracy of the temperature measurements cannot be confirmed. Substantially different temperature histories were recorded at 2 thermocouples situated similarly relative to the laser passes. The lower temperature reading is most likely due to differences in weld size. Due to the very high temperature gradients and fast transients, the presence of the thermocouple on the build plate may alter the local temperature being monitored [19]. Thus, the impact of the thermocouple on the local temperature must be considered in model calibration and validation work.

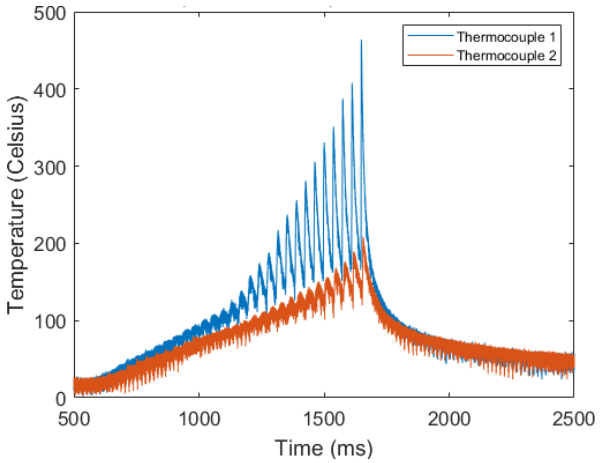

Figure 6. Readings from thermocouples 1 and 2 from test set 6, with a laser power of 400 W, laser speed 2100 mm/s, hatch spacing of 30 *μ*m, and initial and final distances of approximately 900 μm and 30 *μ*m from the thermocouple weld junctions.

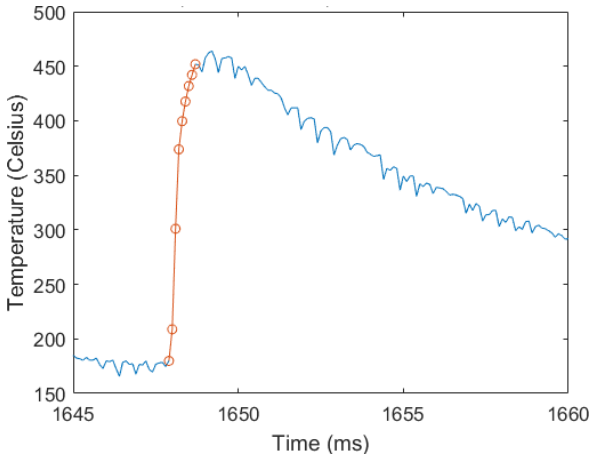

Figure 7. Detail of the highest temperature peak recorded by thermocouple 1 for the same case as shown in figure 6. The red section shows the data points (circles) during the temperature rise.

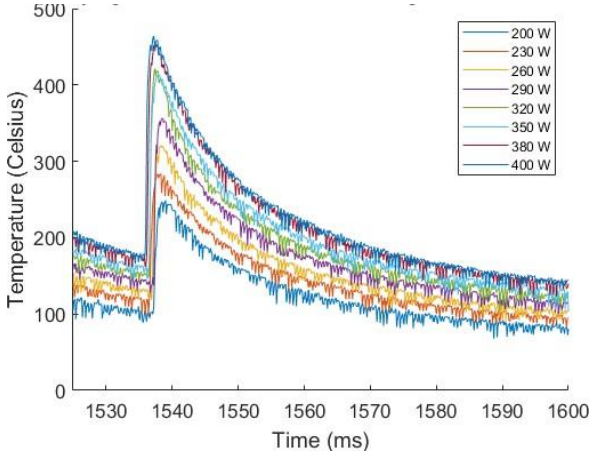

Figure 8. Detail of the final peak from test set 6 (laser speed 2100 mm/s, hatch spacing 30 *μ*m) at different power levels.

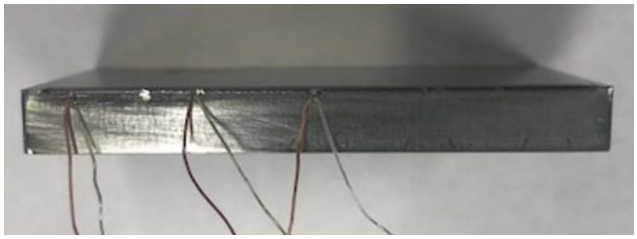

Figure 9. Thermocouples spot welded to the top edge of a 50.8 mm x 25.4 mm x 6.35 mm Inconel 718 build plate for future work.

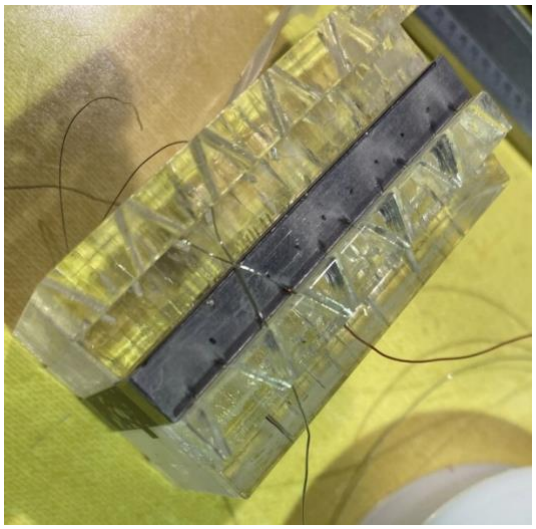

Figure 10. Fixtures for ensuring accurate location of thermocouple weld placement on the build plate.

Future work should include studies including powder and multi-layer builds. A new design has already been proposed, where the thermocouples are mounted on the edge of a half-size build plate

(25.4 mm × 50.8 mm × 6.35 mm) that would be mounted on a full size build plate, rather than in channels on the top of the build plate, as shown in Figure 9. This design keeps the wires away from the powder and rake, the thermocouples are less likely to be damaged as they are not on the surface where the laser passes, and the geometry is easier to model to compare with simulations. It is also relatively easy to grind the edge before reattachment for subsequent experiments. Fixtures have been created to ensure the accurate location of the thermocouples (Figure 10). Future work should also include completing simulations and experiments for direct comparison. If further speedups are desired, the AD8495 thermocouple amplifier is the limiting factor. Improvement of this component would allow further increase in the data acquisition rate.

Acknowledgements

This work was supported by an Early Stage Innovations grant from NASA's Space Technology Research Grants Program under Grant No. 80NSSC18K0256.

References

[1] T. Vilaro, C. Colin, J. Bartout, L. Nazé, and M. Sennour, "Microstructural and mechanical approaches of the selective laser melting process applied to a nickel-base superalloy," *Materials Science and Engineering: A*, vol. 534, pp. 446–451, 2012.

[2] M. F. Zäh and S. Lutzmann, "Modelling and simulation of electron beam melting," *Production Engineering*, vol. 4,no. 1, p. 15–23, 2009.

[3] S. Roy, M. Juha, M. S. Shephard, and A. M. Maniatty, "Heat transfer model and finite element formulation for simulation of selective laser melting," *Computational Mechanics*, vol. 62, no. 3, pp. 273–284, 2018.

[4] J.-W. Ahn, R. Maingi, D. Mastrovito, and A. Roquemore, "High speed infrared camera diagnostic for heat flux measurement in nstx," *Review of Scientific Instruments*, vol. 81, no. 2, p. 023501, 2010.

[5] T. Vilaro, C. Colin, J. Bartout, L. Nazé, and M. Sennour, "Approximation of absolute surface temperature measurements of powder bed fusion additive manufacturing technology using in situ infrared thermography," *Additive Manufacturing*, vol. 5, pp. 31–39, 2015.

[6] J. Raplee, A. Plotkowski, M. Kirka, R. Dinwiddie, Okello, R. Dehoff, and S. Babu, "Thermographic microstructure monitoring in electron beam additive manufacturing," *Scientific Reports*, vol. 7, p. 43554, 03 2017.

[7] H. Krauss, C. Eschey, and M. Zaeh, "Thermography for monitoring the selective laser melting process," in *23rd Annual International Solid Freeform Fabrication Symposium - An Additive Manufacturing Conference, SFF 2012*,(Austin, TX, United states), pp. 999–1014, 2012.

[8] Z. Y. Chua, I. H. Ahn, and S. K. Moon, "Process monitoring and inspection systems in metal additive manufacturing: Status and applications," *International Journal of Precision Engineering and Manufacturing-Green Technology*, vol. 4, no. 2, p. 235–245, 2017.

[9] P. A. Hooper, "Melt pool temperature and cooling rates in laser powder bed fusion," *Additive Manufacturing*, vol. 22, pp. 548–559, 2018.

[10] W. Devesse, D. De Baere, and P. Guillaume, "High resolution temperature measurement of liquid stainless steel using hyperspectral imaging," *Sensors (Switzerland)*, vol. 17, no. 1, 2017.

[11] M. Pavlov, M. Doubenskaia, and I. Smurov, "Pyrometricanalysis of thermal processes in slm technology," *Physics Procedia*, vol. 5, pp. 523–531, 2010. Laser Assisted Net Shape Engineering 6, Proceedings of the LANE 2010, Part 2.

[12] Y. Chivel and I. Smurov, "On-line temperature monitoring in selective laser sintering/melting," *Physics Procedia*, vol. 5, pp. 515–521, 2010.

[13] M. Masoomi, S. Thompson, N. Shamsaei, A. Elwany, and L. Bian, "An experimental-numerical investigation of heat transfer during selective laser melting," in *Proceedings - 26th Annual International Solid Freeform Fabrication Symposium - An Additive Manufacturing Conference, SFF 2015*, pp. 229 – 242, 2020.

[14] M. Chiumenti, X. Lin, M. Cervera, W. Lei, Y. Zheng, and W. Huang, "Numerical simulation and experimental calibration of additive manufacturing by blown powder technology. Part I: thermal analysis," *Rapid Prototyping Journal*, vol. 23, pp. 448–463, 2017.

[15] D. St-Pierre, "AD8495 thermocouple breakout board," 2018. Internal report, Manufacturing Innovation Center, Rensselaer Polytechnic Institute.

[16] "A flexible adaptive open architecture to enable a robust third-party ecosystem for metal powder bed fusion additive manufacturing systems." https://www. americamakes.us/portfolio/4051. Accessed: 2021-05-25.

[17] "Development and demonstration of open-source protocols for powder bed fusion AM." https://www. americamakes.us/portfolio/4039. Accessed: 2021-05-25.

[18] Shkoruta, W. Caynoski, S. Mishra, and S. Rock, "Iterative learning control for power profile shaping in selective laser melting," in *2019 IEEE 15th International Conference on Automation Science and Engineering (CASE),* pp. 655–660, 2019.

[19] M. Attia, A. Cameron, and L. Kops, "Distortion in thermal field around inserted thermocouples in experimental interfacial studies, part 4: End effect," *Journal of Manufacturing Science and Engineering, Transactions of the ASME*, vol. 124, no. 1, pp. 135–145, 2002.

[20] D. St-Pierre, "Thermocouple laser measurement – 3x sensors preliminary data," 2018. Internal report, Manufacturing Innovation Center, Rensselaer Polytechnic Institute.